Effect of Ta Addition on Microstructure and Hot Oxidation Resistance of AlCrCoNiY-xTa High-Entropy Alloy Consolidated by Spark Plasma Sintering

A. Babaei Rouchi[1], A. Salemi Golezani[1,*], S. M. M. Hadavi[2]

[1]Department of Materials Engineering, Karaj Branch, Islamic Azad University, Karaj, Iran.
[2]Department of Materials Engineering, Tarbiat Modares University, Tehran, Iran.
Received: 18 September 2020 - Accepted: 03 December 2020

Abstract

High Entropy Alloys(HAEs) are alloys with multiple elements (typically 5 or more elements) that remain in solid solution state instead of precipitate in several phases. These alloys are multicomponent alloys having constituents in equiatomic or near equiatomic ratios (having the atomic percentage between 5% and 35%). In this paper, the effects of Ta addition on the microstructure and oxidation behavior of 4 High and Medium Entropy Alloys were investigated with the aim of understanding the relationship between phase / microstructure and oxidation resistance of AlCrCoNiY-xTa alloys. The microstructure investigations showed that the presence of Ta alloying element could lead to the formation of $CrTaO_4$ phase. The amount of this phase increases with a higher percentage of Ta element. Also, more results show that, formation of $CrTaO_4$ phase facilitates the formation of Al_2O_3 oxide phase as an outer layer and the presence of this phase can improve the oxidation properties of the investigated alloys.

Keywords: High-Entropy Alloys, Oxidation Resistance, $CrTaO_4$.

1. Introduction

In recent years, there has been a lot of research on a new class of alloys called High-entropy alloys (HEAs). Unlike conventional alloys based on one or two principle elements, high entropy alloys contain at least 5 principle elements each having the atomic percentage between 5% and 35% [1,2]. According to Boltzmann equation [1], increasing the number of components of an alloy leads to an increase in the mixing entropy of the alloy. This increase in mixing entropy enhances the mutual solubility between constituent components and leads to simpler phases and microstructure [3]. HEAs alloys have a combination of Proper mechanical, chemical and electrochemical properties such as high hardness and wear resistance, good strength at high and low temperatures and thermal stability compared to conventional alloys [1-4]. So far, more research on these alloys has focused on mechanical properties and electrochemical properties and less research has been done on oxidation behavior of HEAs [2-5]. One of the important features of HEAs is the Sluggish Diffusion Effect which suggest that diffusion rate in these alloys is lower than conventional alloys [1,4]. According to this effect by increasing the number of elements, the diffusion rate will decrease [6]. Reduced diffusion rates of the alloying elements in high-entropy alloys were attributed to a reduced concentration of free vacancies in these multi-principal-element alloys which could help to control the oxidation [7].

*Corresponding author
Email address: salemiali@gmail.com

Another important feature of HEAs is the Cocktail effect. According to Cocktail effect, as the presence of elements such as Al, Cr, Ti and Hf in conventional alloys can lead to the formation of stable oxides at the alloy surface and improve oxidation resistance; it is also possible in HEAs. For example, the addition of Al and Si in the FeCoNiCr increased the oxidation resistance of the alloy [8]. Also the addition of Ti and Si increased the oxidation resistance of the NbCrMoAl [9]. According to the above, the presence of some elements in HEAs could increase the oxidation resistance. Increasing oxidation resistance and proper mechanical properties could make it possible to use HEAs at high temperature applications. The effect of Ta on oxidation behavior of conventional alloys and super alloys has been investigated and the results show that presence of Ta increases the oxidation resistance of these alloys [10-12]. In this study, the effect of Ta addition on the oxidation properties of AlCrCoNiY alloy was investigated. This alloy system is similar to the MCrAlY-Amdry 995 alloy, made by Oerlikon, which is used as an oxidation resistant coating for hot components of gas turbines. In fact, in this study, using common elements of MCrAlY commercial alloys, some medium and high entropy alloys were fabricated and the effect of Ta addition on them was investigated.

2. Materials and Methods

Four alloys from AlCrCoNiY-xTa fabricated by mechanical alloying using a NARYA-MPM-4*250 planet mill under Ar atmosphere.

Table. 1. Specification of Powders.

Elements	Al	Cr	Co	Ni	Y	Ta
Particle size(µm)	75	44	45	50	420	44
Purity (wt.%)	99.90%	99.00%	99.80%	99.70%	99.50%	99.90%

Table. 2. Nominal composition and configurationally entropy of fabricated alloys.

Alloy	A1		A2		A3		A4	
Element	wt.%	at. %	wt.%	at. %	wt.%	at. %	wt.%	at. %
Al	11.83	22.00	11.35	22.00	10.84	22.00	9.27	20.00
Cr	25.91	25.00	24.85	25.00	23.74	25.00	17.87	25.00
Co	29.36	25.00	28.16	25.00	26.90	25.00	27.35	25.00
Ni	32.46	27.75	29.17	26.00	25.72	24.00	27.24	24.00
Y	0.44	0.25	0.42	0.25	0.41	0.25	0.38	0.25
Ta	0.00	0.00	6.05	1.75	12.39	3.75	17.88	5.75
Total	100.00	100.00	100.00	100.00	100.00	100.00	100.00	100.00
$\Delta S_{conf.}$	1.39697R		1.46227R		1.50687R		1.53001R	

The specification of elemental powders is given in Table. 1. Powders were milled up to 20 hours at 250 RPM with a relaxation time of 15 minutes after each hour. Stearic acid was used as a process control agent to avoid cold welding of particles [13-14]. The milled powders were analyzed using X-ray diffractometer (XRD), scanning electron microscope (SEM) attached with energy dispersive X-ray spectroscope (EDS).

XRD analysis was carried out using Philips PW 1830 set up with Cu-kα radiation (λ=1.540Å) and SEM analysis was carried out by ZEISSE Evo 25 MA25.

The nominal compositions and configurationally entropy of the investigated alloys are given in Table. 2. A1, A2 and A3, A4 are Medium-Entropy and High-Entropy Alloys, respectively.

Spark Plasma Sintering (SPS) process was used for the sintering of alloys. At this method pressing (50 MPa) and sintering (800℃, 10 min) were carried out in one step.

All samples were grinded to mesh 1000, polished by alumina suspensions and etched in Aqua Regia for 60 seconds for microstructural analysis. In oxidation test, samples were cut into pills of 10 mm in diameter and 2 mm thick and grinding up to 1000 mesh and cleaned using ethanol.

Then the samples were oxidized isothermally for 50 hours at 1000 °C. The amount of oxygen absorbed in the samples was measured every 5 hours during oxidation. Oxidized samples were analyzed using XRD, SEM and energy dispersive X-ray spectroscope (EDS).

3. Results and Discussions

SEM images of all samples are shown in Fig. 1. It is clear that by increasing the Ta from A1 to A4, the mixed powder particles have become coarse. EDS analysis confirmed the homogeneity of the chemical composition of the A1 alloy (Fig. 2.a).

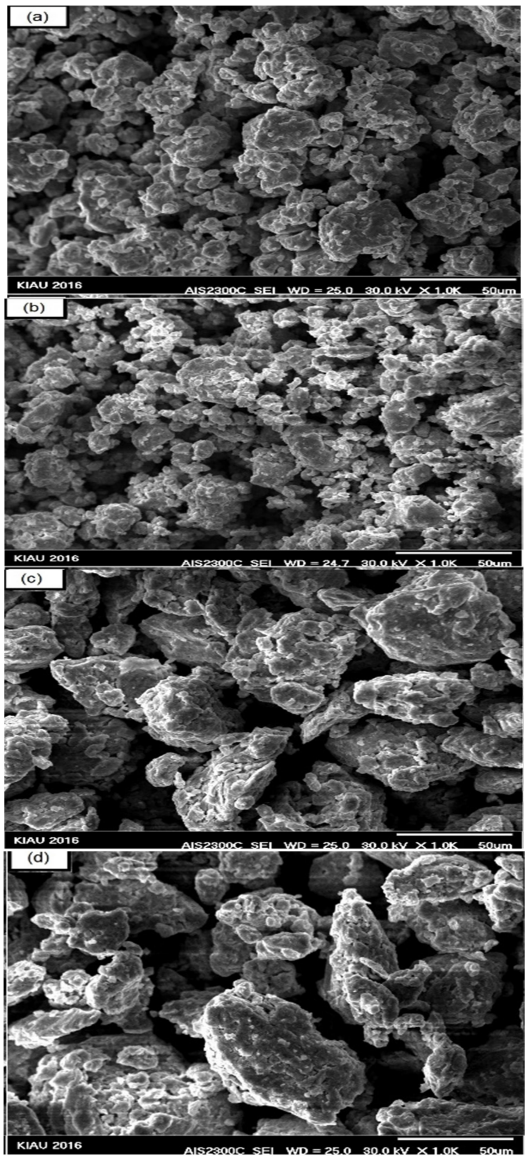

Fig. 1. SEM images of powder alloys (a) A1 alloy (b) A2 alloy (c) A3 alloy (d) A4 alloy.

Also, XRD pattern of this alloy are shown in Fig. 2.b. Removing the peaks related to Al, Co, Ni and Y in the XRD pattern of the A1 alloy means that these elements have been solved in the AlNi lattice [14]. In addition, the existence of AlNi intermetallic compound has been reported for similar alloys [15].

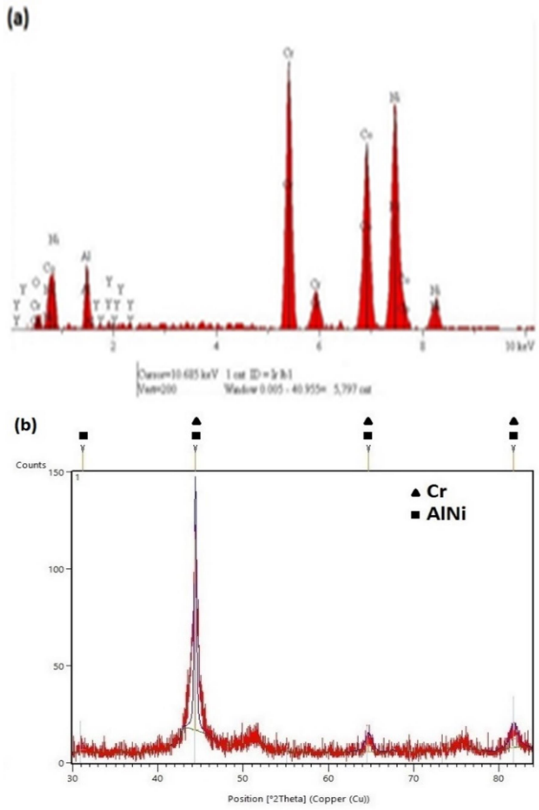

Fig. 2. a) EDS and b) XRD pattern of A1 before sintering.

The XRD pattern of this alloy is similar in angle and peak intensities with AlNi intermetallic compound and Cr XRD pattern. Considering that the AlNi lattice parameter (0.8288 μm) is closer to the lattice parameter of A1 (0.2868 μm) compared to the Cr lattice parameter (28847 μm), it seems that the crystal structure of AlNi is the parent matrix of alloy A1 that other elements in this matrix are soluble [1]. In fact, the A1 alloy is a single-phase solid solution with BCC (B2) structure and other elements are solved in this lattice.

These results are consistent with the results of other researches [16-18]. In the A2 alloy, despite the addition of 1.75 at% Ta to the alloy, the chemical composition is almost homogeneous. The A2 alloy parent matrix is also an AlNi intermetallic compound. The XRD pattern of the A2 alloy is shown in Fig. 3.a. The weak peaks at this pattern can be related to Co_2Ta Laves phase [3]. The AlNi lattice parameter in the A1 alloy (0.2868 μm) is lower than A2 (0.2880 μm) and A3 (0.28484 μm). This indicated that Ta is a key factor in solubility of other elements in AlNi Matrix.

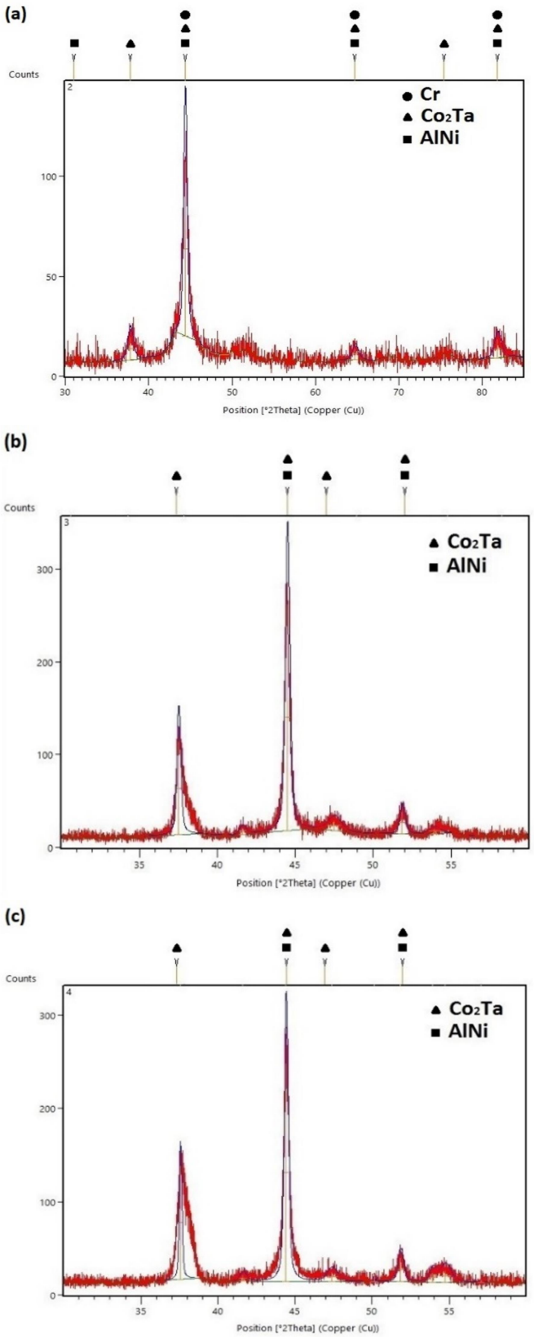

Fig. 3. XRD pattern of a) A2 b) A3 c) A4 alloy.

It seems that the additional Ta amounts, which do not have the ability to dissolve in the AlNi matrix, crystallize in the form of the Co_2Ta Laves phase [19].

In the A3 and A4 alloys, with increasing Ta, more amounts of the Co_2Ta Laves phase are formed. (Fig 3.b, 3.c). The SEM image of the sintered A1, before and after the oxidation is shown in Fig. 4..

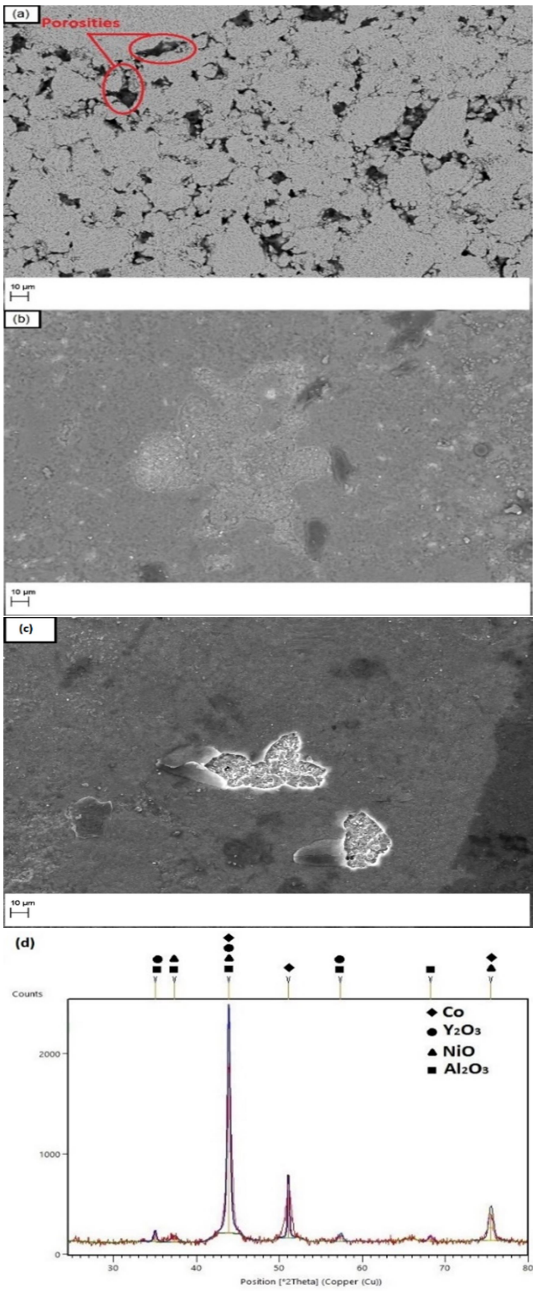

Fig. 4. SEM image of the sintered A1 a) before oxidation b) after oxidation and c) magnified image of A1 oxide surface d) XRD pattern of A1 after oxidation.

There is about 9.64% porosity at the alloy surface before oxidation (Fig. 4a). This amount has reached almost zero after oxidation (Fig. 4b). It can be explained that, the formation of oxide layer at the bottom of the porosities, then the growth and bonding of oxide particles, causes the surface to be covered with oxide layer.

Notable in Fig. 4. is the scaling of the oxide layer in different areas which is shown in Fig. 4.c. The XRD pattern of A1 after oxidation is shown in Fig. 4.d. At this pattern, four reflections can be observed. Intensity of the secondary peak, which is stronger than others, is related to Al_2O_3 phase. Other peaks are related to Co, Y_2O_3 and NiO reflection. According to the thermodynamic and Ellingham diagrams [20-21] Al_2O_3 and Y_2O_3 have the lowest Gibbs free energy at 1000 °C (1273 ° K), therefore the formation of these oxides are thermodynamically preferable compared to the formation of other oxides. In the MCrAlY alloys, which are similar in composition to this alloy, Al_2O_3 oxide layer is reported as the main source of oxidation protection [9,22]. Scanning Electron Microscopy of the A2 alloy is shown in Fig. 5. In this alloy, there was about 8.60% porosity at surface before oxidation, which is less than the A1, also the surface was covered with oxide layers.

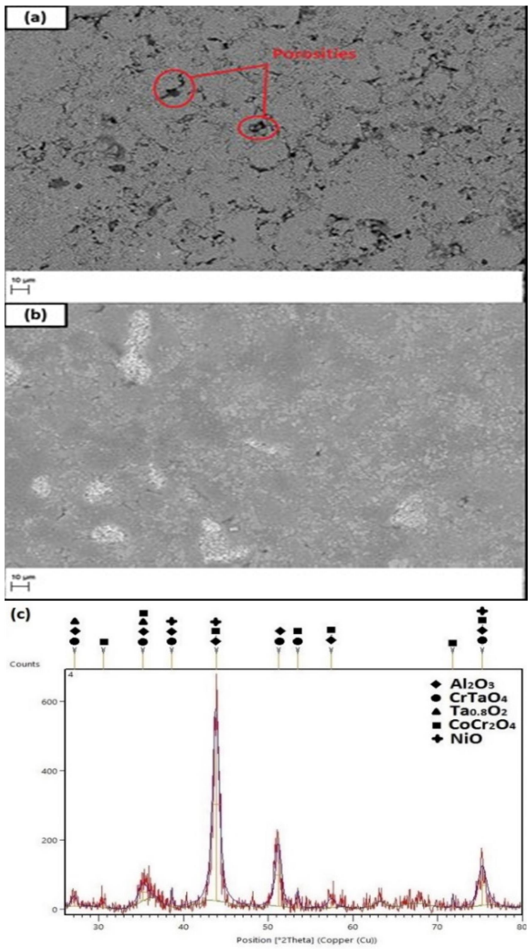

Fig. 5. SEM image of the sintered A2 a) before oxidation b) after oxidation c) XRD pattern of A2 after oxidation.

The oxide layer of A2 alloy composed of a dark and a bright phase which can be seen in detail in Fig. 5b. The dark phase is rich in Al and O elements, which indicate the formation of Al_2O_3. In bright regions, presence of large amounts of Cr, Ta, and O indicate the formation of $CrTaO_4$ in these regions.

The XRD pattern of the A2 alloy which is shown in Fig. 5..c confirms the formation of these two phases.

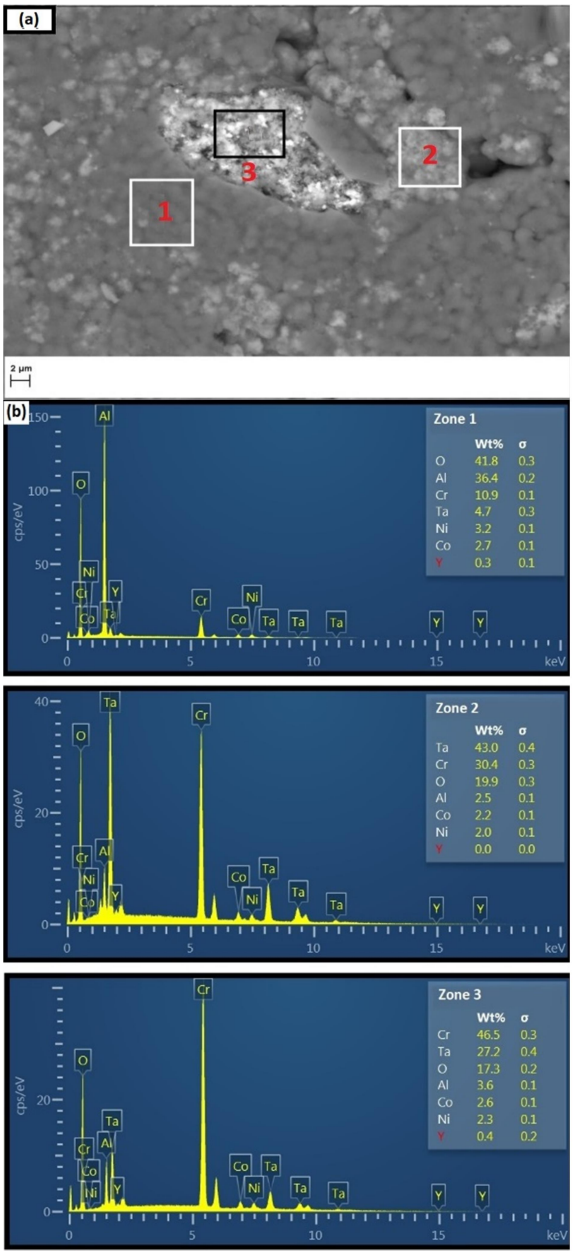

Fig. 6. a) SEM image of the sintered A2 b) EDS pattern of zone 1, 2 and 3.

To reveal the chemical composition changes in the oxide layer, three different areas (marked by the rectangle in Fig. 6.a) of the oxide layer have been chosen to be examined under SEM by EDS patterning and the results are shown in Fig. 6.b.
In Fig. 6.b, the zone 1 (dark phase) was rich in elements of Al and O, which can be effective in the formation of Al_2O_3. In Zone 2 (bright phase), presence of large amounts of Cr, Ta, and O can indicate the formation of $CrTaO_4$. In zone 3, the amount of Al has extremely decreased compared to the nominal composition of the A2 alloy. It seems that Al tends to react with O and withdraw from the AlNi matrix, which causes the formation of the Al_2O_3 phase at surface of sample. Like the A1 alloy, the NiO phase also exists in the A2 alloy. With the addition of Ta to the alloy, in addition to the $CrTaO_4$ phase, the $CoCr_2O_4$ phase is also formed in an alloy that does not exist in the A1 alloy. The low-energy peak of $CoCr_2O_4$ indicate that the amount of this phase is low in the A2 alloy. In the A2 Compared to the A1, there are fewer amounts of Co and Ni in the oxide layer, indicating a lower outward diffusion of these elements from the AlNi matrix.

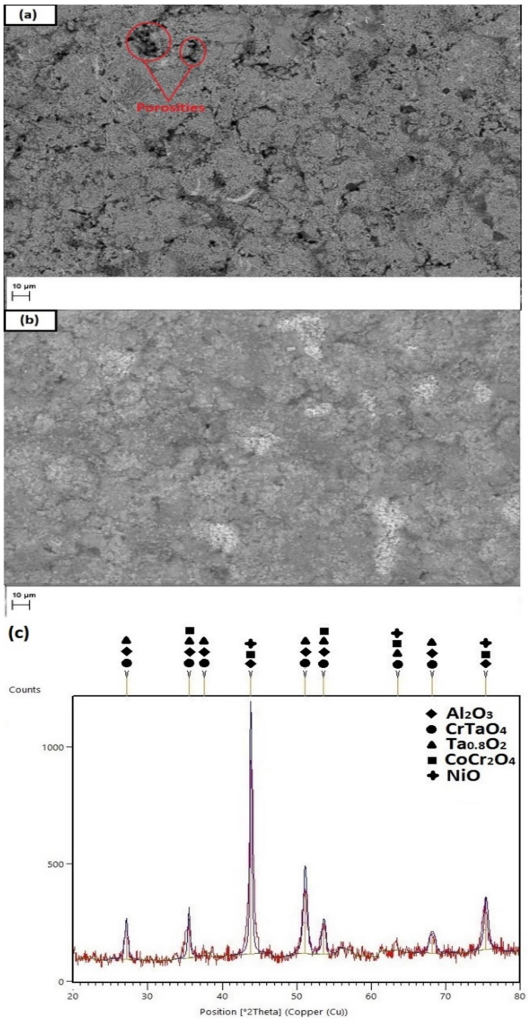

Fig. 7. SEM image of the sintered A3 (a) before, (b) after oxidation and c) XRD pattern of A3 after oxidation.

In samples A3 (Fig. 7.) and A4 (Fig. 8.) the amount of surface porosities before oxidation were obtained 5.67% and 17.39%., respectively. In Fig. 7.b, dark and bright regions are related to Al_2O_3 and $CrTaO_4$, respectively, which is confirmed by EDS and XRD

analysis. As shown in Fig. 7.c, the Intensity of the Al_2O_3, $CrTaO_4$, and $CoCr_2O_4$ peaks have been increased in A3 compared to A2 and It means that the amount of these phases in the A3, are higher than that of the A2 after oxidation. In the A3 alloy, a new phase is formed which is $Ta_{0.8}O_2$. Based on researches conducted on this phase, the Ta_2O_5 phase can be converted to a pseudo-stable rutile-type $Ta_{0.8}O_2$ during heating [23-24]. As shown in Fig. 8.c, the Intensity of the $CrTaO_4$, $Ta_{0.8}O_2$, $CoCr_2O_4$ and Al_2O_3 peaks have been increased in the A4 compared to A3 and It means that the amount of these phases in the A4, are higher than that of the A3 after oxidation.

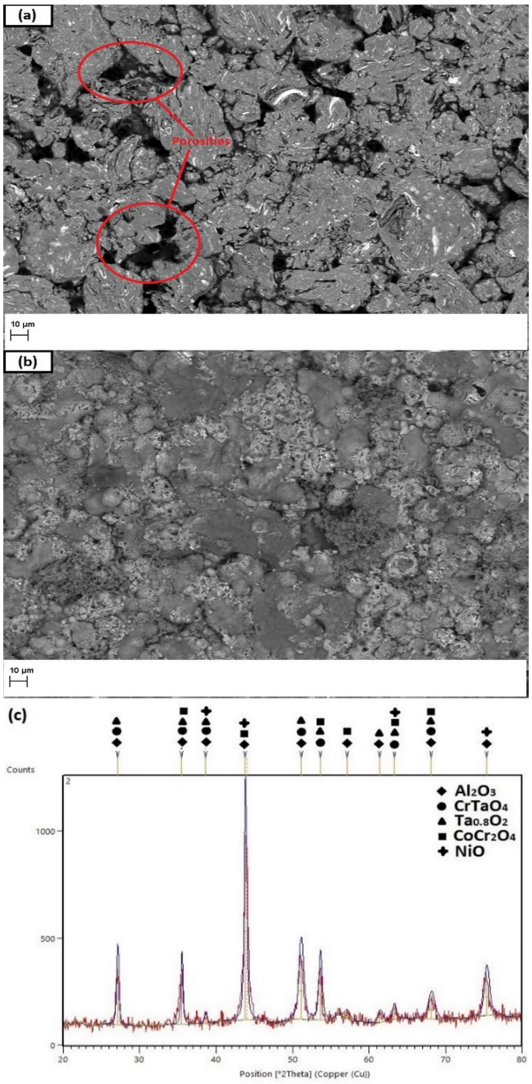

Fig. 8. SEM image of the sintered A4 (a) before, (b) after oxidation and c) XRD pattern of A4 after oxidation.

The results of the oxidation test for alloys A1 to A4 are shown in Fig. 9. According to Fig. 9., the amount of oxygen absorbed in the A1 to A4 alloys are decreased with increasing Ta content.

This reveals that Ta has played an important role in reducing the amount of oxygen absorbed and increasing oxidation resistance.

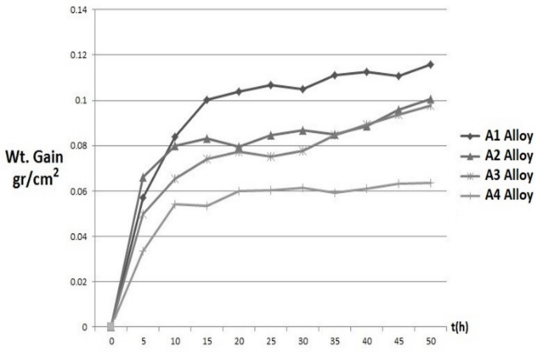

Fig. 9. Oxidation diagram of alloys A1 to A4.

Al_2O_3 is the most important phase for improving oxidation resistance in Superalloys and oxidation-resistant coatings [25]. The formation of an adhesive and continuous Al_2O_3 layer at the alloy surface prevents the diffusion of oxygen into the sub-layers and controls the oxidation of the alloy. As shown in Fig. 9., all samples begin to oxidize rapidly at the beginning of oxidation process. After a while, because of the formation of the Al_2O_3 oxide phase, the oxidation rate decreases in all samples.

In the A1, despite the presence of the Al_2O_3 phase, the alloy exhibits poor oxidation resistance. Insufficient amount of Al_2O_3 phase and low adhesion of the oxide layer could be the main reason of poor oxidation resistance of this alloy [12,25]. As shown in Fig. 4.c, the oxide layer of A1 sample is scaled at different points. This discontinuous layer let the oxygen to diffuse into the substrate and decrease the oxidation resistance of the alloy.

As shown in Fig. 9., the A2 alloy initially oxidizes at high speeds, but the oxidation rate of the alloy decreased after a while due to the formation of Al_2O_3 at sample surface. The A2 alloy also does not exhibit excellent oxidation resistance although it has a better oxidation resistance compared to the A1 alloy. As like the A1 alloy, the low amount of Al_2O_3 phase and insufficient adhesion of the oxide layer to the substrate could be the main reason of poor oxidation resistance of the A2 alloy.

It should be noted that the Al content in this alloy was equal to the alloy A1 but the oxidation resistance was improved. Also the amount of Al_2O_3 phase has increased in this alloy without increasing Al content. The most important differences between the A2 and A1 alloys are the reduction of porosities in the A2 alloy and the presence of Ta in the A2 alloy. Therefore, it seems that the reduction of porosities and the addition of Ta could be the main reason for increasing the amount of Al_2O_3 phase and improving the oxidation resistance of the A2 alloy compared to the A1 alloy.

According to the results in the A4 alloy, despite increasing porosities, oxidation resistance was improved. So it can be concluded that porosities do not have a significant effect on the oxidation resistance of this alloy system and Ta plays the main role in improving the oxidation resistance of these alloys. In the A3 alloy, the intensities of the Al_2O_3 peaks have increased. In this alloy, with increasing Al_2O_3 amount, the amount of absorbed oxygen has decreased, which is shown in Fig. 9. As shown in Fig. 9. in the A4 alloy, the amount of oxygen absorbed is much lower than that of the A1 to A3 alloys. As shown in Fig. 8b, the oxide layer formed on the surface of the A4 alloy is a continuous and adhesive layer.

This makes the alloy more resistant to oxidation than the A1 to A3 alloys. As already mentioned, the intensity of the Al_2O_3 peaks increased in this alloy as shown in Fig. 8c. Due to the fact that the amount of Al in this alloy is lower than that of the A3 alloy, it seems that Ta plays an important role in forming more amounts of the Al_2O_3 phase. The addition of Ta in alloys A2 to A4 has led to the formation of $CrTaO_4$ in these alloys and with increasing Ta content, the amount of this phase also increased in all oxidized samples. Considering that the Al content in alloys A1 to A3 is constant and also decreased in the A4 alloy, it can be concluded that increasing the amount of Al_2O_3 phase in these alloys is directly related to the increase of the Ta content and the $CrTaO_4$ phase. According to studies by other researchers, Ta at low amounts can lead to improved oxidation resistance, but at higher amounts, it can lead to the formation of TaO_2 in the alloy and reduce the stability of the Al_2O_3 phase, thereby reducing oxidation resistance [12]. But according to the results of this study, due to the fact that the alloys were exposed to heat, instead of the TaO_2 phase, the $Ta_{0.8}O_2$ rutile phase was formed through Ta_2O_5 phase transformation and this phase had no negative effect on the oxidation resistance of AlCrCoNiYTa alloy system.

A recent study confirms that the formation of the $CrTaO_4$ can improve the oxidation resistance of alloys [10]. According to the results of this study, the formation of a continuous $CrTaO_4$ layer on the surface of the alloys could help to form a continuous layer of the Al_2O_3 phase below the $CrTaO_4$ layer. In fact, the $CrTaO_4$ layer reduce the outward diffusion of the alloying elements to react with oxygen. Since the size of O atom (0.056 nm) is much smaller than that of Al atom (0.143 nm), O atom can diffuse faster through the $CrTaO_4$ layer than the metal atoms and facilitate the formation of the Al_2O_3 phase below the $CrTaO_4$ layer. So it could be concluded that the formation of higher amount of the Al_2O_3 phase as well as the $CrTaO_4$ phase by adding Ta, is the main reason of improving oxidation resistance in the AlCrCoNiYTa alloy system.

4. Conclusions

Effect of Ta addition on microstructure and hot oxidation resistance of AlCrCoNiYTa High-Entropy Alloy at 1000℃ was studied. The main conclusions are as follows:

1. The continuous $CrTaO_4$ layer is formed on the surface of the alloys by adding Ta to the alloys.
2. Increasing the Ta value increases the oxidation resistance of the alloy. This is due to the formation of more $CrTaO_4$ oxide layer at the alloy surface.
3. The $CrTaO_4$ layer reduce the outward diffusion of the alloying elements to react with oxygen but O atom can diffuse faster through the $CrTaO_4$ layer than the metal atoms and facilitate the formation of the Al_2O_3 phase below the $CrTaO_4$ layer.

References

[1] B.S. Murty, J.W. Yeh, S. Ranganathan, High-Entropy Alloys, Butterworth-Heinemann, 2014
[2] C.b. LIU, Z.M. ZHANG, X.L. JIANG, M. LIU, Z.H. ZHU, Trans. Nonferrous Met. Soc. China, 19(2009), 99.
[3] C.M. Liu, H.M. Wang, S.Q. Zhang, H.B. Tang, A.L. Zhang, J. Alloys Compd., 583 (2014), 162.
[4] D.B. Miracle, O.N. Senkov, Acta Mater., 122 (2017), 448.
[5] H. Jiang, K. Han, D. Qiao, Y. Lu, Z. Cao, T. Li, Mater. Chem. Phys., 210 (2018), 43.
[6] S.M. Howard, Ellingham Diagrams. SD School of Mines and Technology, 2006
[7] J.W. Yeh, S.K. Chen, S.J. Lin, J.Y. Gan, T.S. Chin, T.T. Shun, C.H. Tsau. S.-Y. Chang, Adv. Eng. Mater., 6 (2004), 299.
[8] K.Y. Tsai, M.H. Tsai, J.W. Yeh, Acta Mater., 61 (2013), 4887.
[9] M. Bensch, A. Sato, N. Warnken, E. Affeldt, R.C. Reed, U. Glatzel, Acta Mater., 60 (2012), 5468.
[10] M. Shibata, S. K., Mater. Trans., 47(2006), 1638.
[11] O. N. Senkov, S. V. Senkova, D. M. Dimiduk, C. Woodward, D. B. Miracle, J. Mater. Sci., 47(2012), 6522.
[12] P. Fox, G. J. Tatlock, Mater. Sci. Technol., 5(1989), 816.
[13] T. B. Reed, Free energy of formation of binary compounds. MIT Press, 1972
[14] S. Singh, N. Wanderka, B.S. Murty, U. Glatzel, J. Banhart, Acta Mater., 59(2011), 182.
[15] S.j. Park, S.M. Seo, Y.S. Yoo, H.W. Jeong, H.j. Jang, Corros. Sci., 90(2015), 305.
[16] V. Dolique, A.L. Thomann, P. Brault, Y. Tessier, P. Gillon, Mater. Chem. Phys., 117(2009), 142.
[17] W. Kai, W. L. Jang, R. T. Huang, C. C. Lee, H. H. Hsieh, C. F. Du, Oxid. Met., 63(2005), 169.
[18] W. Ren, F. Ouyang, B. Ding, Y. Zhong, J. Yu, Z. Ren, L. Zhou, J. Alloys Compd., 724(2017), 565.

[19] W.R. Wang, W.L. Wang, J.W. Yeh, Phases, J. Alloys Compd., 589(2014), 143.
[20] Y. Liu, J. Wang, Q. Fang, B. Liu, Y. Wu, S. Chen, Intermetallics, 68(2016), 16.
[21] Y. Syono, M. Kikuchi, T. Goto, K. Fukuoka, J. Solid State Chem., 50(1983), 133.
[22] Y. Zhang, S. G. MaJ. W. Qiao, Metall. Mater. Trans. A, 43(2012), 2625.
[23] Yeh, J.W, Ann. Chim., 31(2006), 633.
[24] Yeh, J.W, JOM, 65(2013), 1759.
[25] Z. Fu, W. Chen, S. Fang, D. Zhang, H. Xiao, D. Zhu, J. Alloys Compd., 553(2013), 316.